

# Novel Four-Pyridylbenzene-Armed Biphenyls as Electron-Transport Materials for Phosphorescent OLEDs

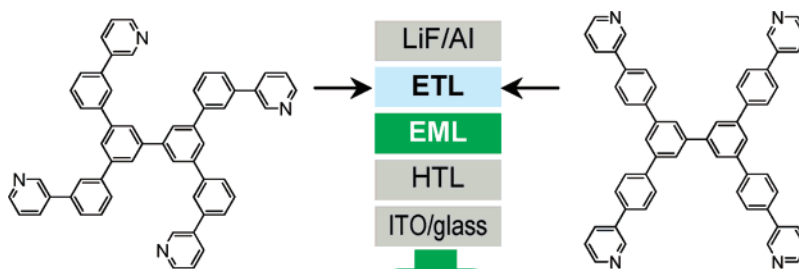
Shi-Jian Su,<sup>\*,†,‡</sup> Daisaku Tanaka,<sup>†</sup> Yan-Jun Li,<sup>†</sup> Hisahiro Sasabe,<sup>†</sup>  
Takashi Takeda,<sup>†</sup> and Junji Kido<sup>\*,†,‡</sup>

Optoelectronic Industry and Technology Development Association, Bunkyo-ku,  
Tokyo 112-0014, Japan, and Department of Polymer Science and Engineering,  
Faculty of Engineering, Yamagata University, 4-3-16 Jonan, Yonezawa,  
Yamagata 992-8510, Japan

sushijian@hotmail.com; kid@yz.yamagata-u.ac.jp

Received December 29, 2007

## ABSTRACT



A series of four-pyridylbenzene-armed biphenyl derivatives were designed and synthesized as an electron-transport and exciton- and hole-block layer for the *fac*-tris(2-phenylpyridine)iridium (*Ir*(PPy)<sub>3</sub>)-based green phosphorescent organic light-emitting devices (OLEDs), giving improved efficiency in comparison to that with both the electron-transport layer of tris(8-hydroxyquinoline)aluminum (Alq3) and the exciton- and hole-block layer of 2,9-dimethyl-4,7-diphenylphenanthroline (BCP).

Since the first report of multilayered organic light-emitting devices (OLEDs),<sup>1</sup> many studies have focused on improving the device efficiency of OLEDs.<sup>2</sup> Recently, phosphorescent OLEDs using phosphorescent dyes doped into charge-transporting hosts as emissive layers (EMLs) have attracted intensive attention due to the highly efficient emission compared to conventional fluorescent OLEDs, through radiative recombination of both singlet and triplet excitons.<sup>3</sup>

Triplets typically have long diffusion lengths.<sup>4</sup> To prevent exciton quenching by the electron-transport layer (ETL) and hole leakage into the ETL, an exciton- and/or hole-block layer was generally inserted between the EML and ETL,<sup>3c,5</sup> and it was reported that no efficient emission can be obtained if there is not a hole- and exciton-block layer, which has electron-transport properties.<sup>3b,6</sup> This may induce more complexity of device structure and thus higher cost for applications to flat-panel displays and lighting. As such, it

<sup>†</sup> Optoelectronic Industry and Technology Development Association.

<sup>‡</sup> Yamagata University.

(1) Tang, C. W.; Vanslyke, S. A. *Appl. Phys. Lett.* **1987**, *51*, 913.

(2) (a) Kido, J.; Iizumi, Y. *Appl. Phys. Lett.* **1998**, *73*, 2721. (b) Okumoto, K.; Kanno, H.; Hamada, Y.; Takahashi, H.; Shibata, K. *Appl. Phys. Lett.* **2006**, *89*, 063504.

(3) (a) Baldo, M. A.; O'Brien, D. F.; You, Y.; Shoustikov, A.; Sibley, S.; Thompson, M. E.; Forrest, S. R. *Nature (London)* **1998**, *395*, 151. (b) Baldo, M. A.; Lamansky, S.; Burrows, P. E.; Thompson, M. E.; Forrest, S. R. *Appl. Phys. Lett.* **1999**, *75*, 4. (c) Watanabe, S.; Ide, N.; Kido, J. *Jpn. J. Appl. Phys.* **2007**, *46*, 1186. (d) Tanaka, D.; Sasabe, H.; Li, Y.-J.; Su, S.-J.; Takeda, T.; Kido, J. *Jpn. J. Appl. Phys.* **2007**, *46*, L10.

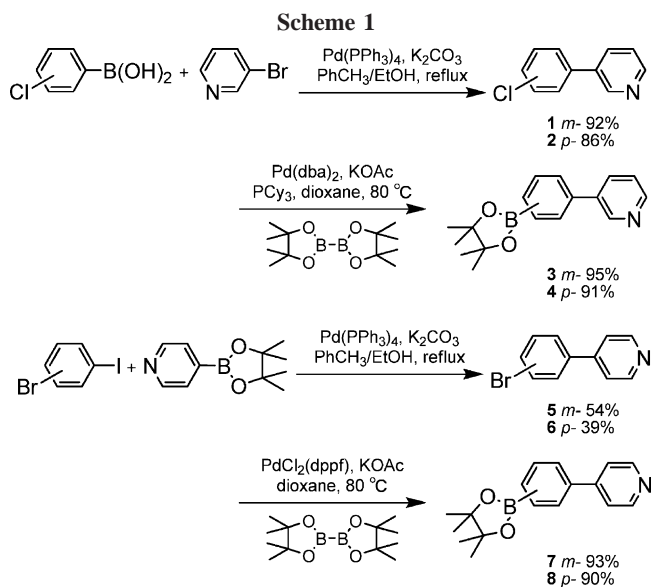
(4) (a) Baldo, M. A. *Phys. Rev. B* **1999**, *66*, 14422. (b) Sun, Y.; Giebink, N. C.; Kanno, H.; Ma, B.; Thompson, M. E.; Forrest, S. R. *Nature (London)* **2006**, *440*, 908.

(5) (a) Ikai, M.; Tokito, S.; Sakamoto, Y.; Suzuki, T.; Taga, Y. *Appl. Phys. Lett.* **2001**, *79*, 156. (b) He, G.; Pfeiffer, M.; Leo, K.; Hofmann, M.; Birnstock, J.; Pudzich, R.; Salbeck, J. *Appl. Phys. Lett.* **2004**, *85*, 3911. (c) Watanabe, S.; Agata, Y.; Tanaka, D.; Kido, J. *J. Photopolym. Sci. Technol.* **2005**, *18*, 83.

(6) Adachi, C.; Baldo, M. A.; Forrest, S. R.; Thompson, M. E. *Appl. Phys. Lett.* **2000**, *77*, 904.

becomes particularly challenging to develop electron-transport materials (ETMs) that can also act as an exciton- and hole-block layer. The object ETM should possess an appropriate lowest unoccupied molecular orbital (LUMO) level to give a low electron injection barrier, a low-lying highest occupied molecular orbital (HOMO) level to block holes from EML, and a high triplet energy level to block triplet excitons formed in the EML. To match these requirements, the conjugation length of the ETM must be extremely confined to achieve a wide energy gap and a high triplet energy ( $E_T$ ) level. It is well-known that the  $\pi$ -electron delocalizations are extended along the elongated molecular axis for para linkage with  $E_T$  decreasing with the number of phenyl and interrupted at the meta linkage.<sup>7</sup> As an example, the  $E_T$  of *m*-terphenyl (2.81 eV) is close to that of biphenyl (2.84 eV) and much higher than that of *p*-terphenyl (2.55 eV).<sup>8</sup>  $E_T$  of a typical phosphorescent emitter of *fac*-tris(2-phenylpyridine) iridium (Ir(PPy)<sub>3</sub>) is 2.55 eV. It seems that a molecule with a  $\pi$ -electron delocalization longer than *p*-terphenyl might not be appropriate to block its triplet excitons formed in the EML for the Ir(PPy)<sub>3</sub>-based phosphorescent OLEDs. To give an ETM with improved electron mobility, heteroaromatics like phenanthroline,<sup>9</sup> pyridine,<sup>10</sup> pyrimidine,<sup>11</sup> quinoline,<sup>12</sup> triazole,<sup>13</sup> etc. were incorporated into the  $\pi$ -conjugated systems. However, more delocalized  $\pi$ -conjugation may induce a narrower energy gap and a lower triplet energy level.

We report in this letter syntheses of a series of four-pyridylbenzene-armed biphenyls with controlled  $\pi$ -conjugation and application for the Ir(PPy)<sub>3</sub>-based green phosphorescent OLEDs as an electron-transport and exciton- and hole-block layer. Device efficiency was improved significantly in comparison to the devices with both electron-transport and exciton- and hole-block layers. They were designed and synthesized by introducing pyridyls on the periphery of the molecules started from bromopyridine or pyridylboronate. All the pyridyls and phenyls were combined with each other at the meta position for **10a** and **10b** in comparison to **11a** and **11b** which contain a more elongated  $\pi$ -conjugation of 4-pyridyl-1,1'-biphenyl. Scheme 1 shows synthetic routes of pinacol boronates of pyridylbenzene. Pyrid-3-yl-containing **1** and **2** were synthesized by Suzuki–Miyaura coupling reaction between chlorophenylboronic acid and 3-bromopyridine in high yields. In comparison, pyrid-4-yl-containing **5** and **6** were synthesized from bromiodo-



benzene and pinacol pyrid-4-ylboronate in a moderate yield. Cross-coupling reaction of bis(pinacolato)diboron with **1** and **2** catalyzed by bis(dibenzylideneacetone) palladium(0) (Pd(dba)<sub>2</sub>) with the ligand of tricyclohexylphosphine (PCy<sub>3</sub>) gives the corresponding arylboronates of **3** and **4** in the presence of potassium acetate, respectively.<sup>14</sup> Pyrid-4-yl-containing arylboronates of **7** and **8** were synthesized by a modified cross-coupling reaction of bis(pinacolato)diboron with **5** and **6** catalyzed by 1,1'-bis(diphenylphosphino)-ferrocene dichloropalladium(II) (PdCl<sub>2</sub>(dppf)).<sup>15</sup>

3,3',5,5'-Tetrabromobiphenyl (**9**) was synthesized by the lithiation of 1,3,5-tribromobenzene followed by oxidative coupling with CuCl<sub>2</sub>.<sup>16</sup> Following Suzuki–Miyaura coupling reaction of **9** with arylboronates of **3**, **4**, **7**, and **8** gives 3,5,3',5'-tetra(*m*-pyrid-3-yl)phenyl[1,1']biphenyl (**10a**), 3,5,3',5'-tetra(*p*-pyrid-3-yl)phenyl[1,1']biphenyl (**11a**), 3,5,3',5'-tetra(*m*-pyrid-4-yl)phenyl[1,1']biphenyl (**10b**), and 3,5,3',5'-tetra(*p*-pyrid-4-yl)phenyl[1,1']biphenyl (**11b**), respectively (Scheme 2).

As shown in Table 1, HOMO levels of both the pyrid-3-yl- and pyrid-4-yl-containing biphenyl derivatives determined by atmospheric ultraviolet photoelectron spectroscopy are around 6.60 eV. They are much lower than that of well-known ETM of tris(8-hydroxyquinoline)aluminum (Alq<sub>3</sub>)<sup>5a</sup> and equal to that of well-known hole-block material of 2,9-dimethyl-4,7-diphenylphenanthroline (BCP),<sup>6</sup> indicating their improved hole-block property. LUMO levels of **10a** and **10b** calculated from their HOMO levels and the lowest energy absorption edges of the UV–vis absorption spectra are 2.57 and 2.53 eV, respectively, in contrast to 2.94 and 3.04 eV for **11a** and **11b**. Much lower lying LUMO levels for **11a**

(7) Brike, J. B. *Photophysics of Aromatic Compounds*; John Wiley & Sons: New York, 1970.

(8) (a) Higuchi, J.; Hayashi, K.; Yagi, M.; Kondo, H. *J. Phys. Chem. A* **2002**, *106*, 8609. (b) Higuchi, J.; Hayashi, K.; Seki, K.; Yagi, M.; Ishizu, K.; Kohno, M.; Ibuki, E.; Tajima, K. *J. Phys. Chem. A* **2001**, *105*, 6084.

(9) Naka, S.; Okada, H.; Onnagawa, H.; Tsutsui, T. *Appl. Phys. Lett.* **2000**, *76*, 197.

(10) (a) Yamamoto, T.; Maruyama, T.; Zhou, Z.-H.; Ito, T.; Fukuda, A.; Kubota, K. *J. Am. Chem. Soc.* **1994**, *116*, 4832. (b) Tamao, K.; Uchida, M.; Izumizawa, T.; Furukawa, K.; Yamaguchi, S. *J. Am. Chem. Soc.* **1996**, *118*, 11974.

(11) Wong, K.-T.; Hung, T. S.; Lin, Y. T.; Wu, C.-C.; Lee, G.-H.; Peng, S.-M.; Chou, C. H.; Su, Y. O. *Org. Lett.* **2002**, *4*, 513.

(12) Saito, N.; Kanbara, T.; Nakamura, Y.; Yamamoto, T.; Kubota, K. *Macromolecules* **1997**, *27*, 657.

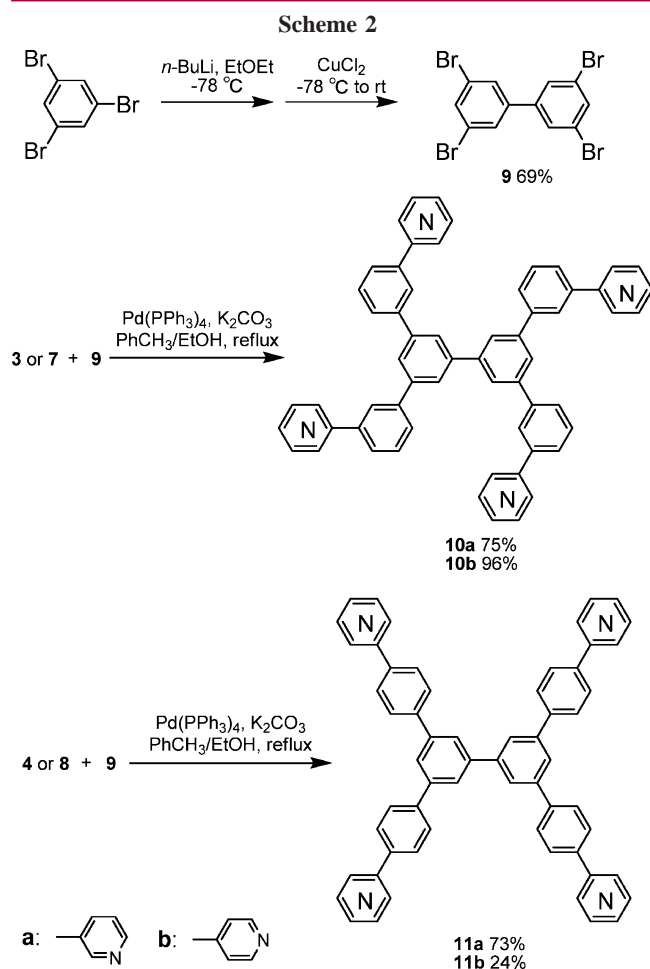
(13) (a) Kido, J.; Hongawa, K.; Okuyama, K.; Nagai, K. *Appl. Phys. Lett.* **1994**, *64*, 815. (b) Kido, J.; Kimura, M.; Nagai, K. *Chem. Lett.* **1996**, 47.

(14) Ishiyama, T.; Ishida, K.; Miyaura, N. *Tetrahedron* **2001**, *57*, 9813.

(15) (a) Ishiyama, T.; Miyaura, N. *J. Organomet. Chem.* **2000**, *611*, 392.

(b) Ishiyama, T.; Itoh, Y.; Kitano, T.; Miyaura, N. *Tetrahedron Lett.* **1997**, *38*, 3447. (c) Ishiyama, T.; Murata, M.; Miyaura, N. *J. Org. Chem.* **1995**, *60*, 7508.

(16) Yamanai, Y.; Sakamoto, Y.; Kusukawa, T.; Fujita, M.; Sakamoto, S.; Yamaguchi, K. *J. Am. Chem. Soc.* **2001**, *123*, 980.



and **11b** arising from their more delocalized  $\pi$ -conjugation may induce a lower electron-injection barrier. In addition,

**Table 1.** Physical Properties of **10a,b** and **11a,b**

materials	HOMO <sup>a</sup> (eV)	LUMO <sup>b</sup> (eV)	$\lambda_{\text{max}}^c$ (nm)	$T_g^d$ (°C)	$T_m^d$ (°C)	$T_d^e$ (°C)
<b>10a</b>	6.66	2.57	258, 357	107	191	503
<b>10b</b>	6.67	2.53	262, 358	128	265	505
<b>11a</b>	6.58	2.94	293, 372		319	523
<b>11b</b>	6.68	3.04	298, 391		382	500

<sup>a</sup> Determined by atmospheric ultraviolet photoelectron spectroscopy. <sup>b</sup> Calculated from the HOMO level and the lowest energy absorption edge of the UV-vis absorption spectrum. <sup>c</sup> Absorption and photoluminescent spectra in vacuum deposited film on quartz substrate. <sup>d</sup> Glass transition temperature ( $T_g$ ) and melting temperature ( $T_m$ ) obtained from differential scanning calorimetry (DSC) measurement. **11a** and **11b** crystallized during the heating-cooling cycles, and no  $T_g$  was detected for them. <sup>e</sup> Decomposition temperature ( $T_d$ ) obtained from thermogravimetric analysis (TGA).

all-meta-combined **10a** and **10b** have relatively high glass transition temperatures ( $T_g$ ), proving the high morphologic stability of the amorphous phase in a deposited film, which is a prerequisite for the application in OLEDs.  $T_g$  of pyrid-4-yl-containing **10b** is 20 °C higher than that of pyrid-3-yl-containing **10a** due to its higher polarity and thus stronger molecular interactions.

To confirm their triplet exciton confinement property, the transient photoluminescence decay of 3% (by weight) Ir-(PPy)<sub>3</sub> doped into typical four-pyridylbenzene-armed biphenyls of **10a** and **11a** was measured (Figure 1). As expected,

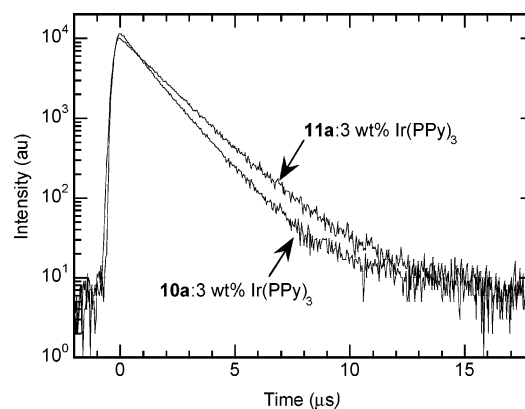


**Figure 1.** Transient photoluminescence decay curves of **10a**:3 wt % Ir(PPy)<sub>3</sub> and **11a**:3 wt % Ir(PPy)<sub>3</sub> under excitation by a nitrogen laser ( $\lambda = 337$  nm, 50 Hz, 800 ps pulses) at rt.

both the **10a**:Ir(PPy)<sub>3</sub> and **11a**:Ir(PPy)<sub>3</sub> films exhibit almost monoexponential decays with relatively long lifetimes of 1.26 and 1.58  $\mu\text{s}$ , respectively, indicating the triplet energy transfer from Ir(PPy)<sub>3</sub> to **10a** and **11a** was successfully suppressed to confine the triplet excitons on the guest molecules.<sup>17</sup> This is of importance as an exciton-block layer to confine triplet excitons in the EML leading to highly efficient phosphorescent OLEDs.

To evaluate their electron-transport and hole- and exciton-block properties, green phosphorescent OLEDs based on Ir-(PPy)<sub>3</sub> were fabricated with **10a** and **11a** as an ETL without inserting any hole- or exciton-block layers between EML and ETL. Poly(arylene amine ether sulfone)-containing tetraphenylbenzidine (TPDPES) doped with 10 wt % tris-(4-bromophenyl)aminium hexachloroantimonate (TBPAAH) was spun onto the precleaned indium-tin oxide (ITO)-coated glass substrate from its dichloroethane solution to form a 20-nm-thick polymer buffer layer.<sup>18</sup> Then, a 30-nm-thick hole transport layer of 1,1-bis[4-[*N,N*-di(*p*-tolyl)amino]phenyl]-cyclohexane (TAPC) was deposited. Next, 7 wt % Ir(PPy)<sub>3</sub> was co-deposited with *N,N'*-dicarbazolyl-4,4'-biphenyl (CBP) to form the 10-nm-thick EML. Finally, a 50-nm-thick ETL consisting of either **10a** or **11a** was deposited to block holes and to confine triplet excitons in the emissive zone. For comparison, a device with BCP as the hole- and exciton-block layer (10 nm) and Alq3 as the ETL (40 nm) was also fabricated. Cathodes consisting of a 0.5-nm-thick layer of LiF followed by a 100-nm-thick layer of Al were patterned using a shadow mask with an array of 2 mm  $\times$  2 mm openings.

(17) Baldo, M. A.; Adachi, C.; Forrest, S. R. *Phys. Rev. B* **2000**, 62, 10967.

(18) (a) Sato, Y.; Ogata, T.; Kido, J. *Proc. SPIE* **2000**, 4105, 134. (b) Fukase, A.; Dao, K. L. T.; Kido, J. *Polym. Adv. Technol.* **2002**, 13, 601.

Their current density versus driving voltage characteristics (Figure 2) indicate that the driving voltages of the devices

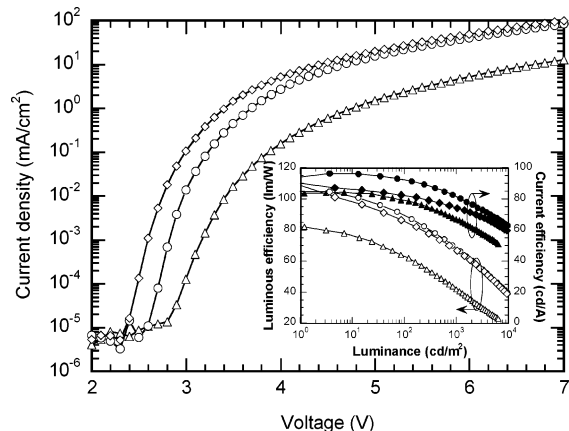


**Figure 2.** Current density vs driving voltage characteristics for ITO/TPDPES:TBPAH (20 nm)/TAPC (30 nm)/CBP:7 wt % Ir(PPy)<sub>3</sub> (10 nm)/**10a** (circles) or **11a** (diamonds) (50 nm)/LiF (0.5 nm)/Al (100 nm) and ITO/TPDPES:TBPAH (20 nm)/TAPC (30 nm)/CBP:7 wt % Ir(PPy)<sub>3</sub> (10 nm)/BCP (10 nm)/Alq3 (40 nm)/LiF (0.5 nm)/Al (100 nm) (triangles). Inset: efficiency vs luminance characteristics.

based on **10a** and **11a** are much lower than that of the device based on BCP and Alq3. The LUMO level of **10a** is slightly higher than those of CBP (−2.7 eV) and Ir(PPy)<sub>3</sub> (−2.8 eV),<sup>5a</sup> facilitating efficient electron transfer from the ETL to the EML. In contrast, the LUMO level of BCP is 0.3 eV lower than that of CBP and 0.2 eV lower than that of Ir(PPy)<sub>3</sub>, and it may induce an electron injection barrier between the EML and the hole- and exciton-block layer of BCP. The driving voltage of the **11a**-based device further decreased due to its lower lying LUMO level and more delocalized  $\pi$ -conjugation, which may induce an increased electron-injection and transport. Besides their appropriate LUMO levels, the coordination effect of the nitrogen atom in periphery pyridyls with lithium cations may also induce an effective electron injection and thus a low driving voltage.<sup>19</sup> Peak current efficiencies of 96.5 and 90.2 cd/A were obtained for **10a**- and **11a**-based devices, respectively, which are higher than that of the device based on BCP and

Alq3 (84.4 cd/A) and those of the previously reported devices based on both ETL and hole- and exciton-block layers (Figure 2, inset).<sup>3b,5,6</sup> At the practical brightness of 100 cd/m<sup>2</sup>, their current efficiencies remain at 92.6 and 82.4 cd/A, respectively, which are higher than that of the device based on BCP and Alq3 (79.2 cd/A). Much higher luminous efficiencies of 89.8 and 85.9 lm/W were achieved at 100 cd/m<sup>2</sup> for **10a**- and **11a**-based devices, respectively, due to increased carrier balance and decreased driving voltage, which are even higher than that of the device with an *n*-doping ETL and an exciton-block layer.<sup>5b</sup> At a much brighter emission of 1000 cd/m<sup>2</sup>, their luminous efficiencies remain at 68.5 and 67.2 lm/W, respectively, which are even higher than that of the device based on BCP and Alq3 at a low luminance of 100 cd/m<sup>2</sup>. It is quite interesting that their current efficiency remains over 60 cd/A even when the brightness reaches 9000 cd/m<sup>2</sup>. The reduced efficiency roll-off at a high current density should arise from the balanced injection of both holes and electrons and the efficient confinement of triplet excitons generated in the EML. Moreover, no emission from **10a** and **11a** was observed in the electroluminescent (EL) spectra, further proving that holes and excitons are well confined within the EML by the current ETMs.

In conclusion, a series of four-pyridylbenzene-armed biphenyls were designed and synthesized as ETMs for efficient green phosphorescent OLEDs. Our findings indicate that highly efficient emission can be achieved with finely designed ETMs as a single ETL instead of generally used ETL combined with hole- and exciton-block layers. Further modification of the central skeleton to create other pyridylbenzene-containing ETMs from the pinacol boronates of pyridylbenzene developed here to finely tune their energy levels and carrier mobility and exploration of their structure-performance correlation are currently under investigation and will be reported in due course.

**Acknowledgment.** This work was financially supported by the New Energy and Industrial Technology Development Organization (NEDO) through the “Advanced Organic Device Project”.

**Supporting Information Available:** Experimental procedures, analytical and spectroscopic data of compounds, UV–vis and PL spectra of **10a,b** and **11a,b**, device fabrication, and summary of device characteristics. This material is available free of charge via the Internet at <http://pubs.acs.org>.

OL7030872

(19) Oyamada, T.; Yoshizaki, H.; Sasabe, H.; Adachi, C. *Chem. Lett.* **2004**, 33, 1034.